The Movement of tRNA Through the Ribosome

Joachim Frank*# and Rajendra K. Agrawal*
*Wadsworth Center, New York State Department of Health, and #Department of Biomedical Sciences, State University of New York at Albany, Empire State Plaza, Albany, New York 12201-0509 USA

ABSTRACT The interaction between tRNA and the ribosome during translation, specifically during elongation, constitutes an example of the motion and adaptability of living molecules. Recent results obtained by cryoelectron microscopy of "naked" ribosomes and ribosomes in functional binding states shine some light on this fundamental life-sustaining process. Inspection of the surface contour of our reconstruction reveals a precise "lock-and-key" fit between the intersubunit space and the tRNA molecule.

INTRODUCTION

The recent publication of cryomaps with greatly improved resolution (Frank et al., 1995a,b; Stark et al., 1995) over that of the earlier cryomap (Frank et al., 1991) marks a turning point in the struggle to gain insight into the complex structure of the ribosome, and to unravel the way in which it interacts with its substrate molecules. This article will focus on what we have learned thus far about the interactions between the ribosome and tRNA in the course of the elongation cycle, especially by using the technique of cryoelectron microscopy (cryo-EM).

The elongation phase of protein biosynthesis is a complex multistep process, involving the ribosome, mRNA, tRNAs, and various protein factors, by which a new amino acid is added to the growing polypeptide chain. In this process, the coordinated movement of tRNA through the ribosome, during which it interacts with various binding sites, plays a pivotal role.

A physical model of our ribosome cryomap (Frank et al., 1995b), made by Manjuli Sharma in this laboratory, strikingly demonstrates the extent to which the ribosome is adapted to accommodate the movement of the tRNA molecule through its intersubunit space. To put the observation into a succinct form, the shape of the intersubunit space looks, to a first approximation, as though it might have been punched out by a tRNA-shaped cookie cutter from a clump of dough. There are several cross-sections of this space, apparent by viewing the model from different angles, that make allowance for the elbow-shaped tRNA molecule. The fit is nearly perfect if one allows the volume to expand to nearly 4×10^6 Å^3 (see Fig. 1), although that volume represents a 1.5-fold increase over the volume computed from the chemical mass of protein and RNA constituents (2.6×10^6 Å^3; see, e.g., Stark et al., 1995). Before describing the spatial constraints of tRNA-ribosome interaction, it is useful to discuss the rationales underlying the choice of the ribosome's molecular envelope.

THE MOLECULAR ENVELOPE OF THE RIBOSOME

Despite the striking agreement in many features between the maps presented by the two groups (see Moore, 1995), the difference in the overall appearance of the structure has produced some puzzlement. Whereas the reconstruction by Frank and co-workers (1995b) (displayed with a threshold encompassing 3.4×10^6 Å^3, or a 1.3-fold increase over the chemical mass) looks quite compact, the one by Stark and co-workers (1995) (using 2.9×10^6 Å^3) appears rather open and fragmented, almost "Swiss-cheese"-like.

The appearance of the ribosome is influenced by two effects. One is the choice of cutoff threshold (which is conveniently parameterized in terms of the volume included), the other the degree to which low spatial-frequency components of the original structure are correctly rendered in the 3D map. The two effects act in concert, because with either under- or overrepresented low spatial frequencies, there is no guarantee that the known volume will lead to a sensible threshold, or that the relative values of densities in points separated by a large distance are correct (see Frank, 1996). The compact appearance of the ribosome map of Frank and co-workers reflects the choice of a volume somewhat larger than the chemical-mass volume, as well as the effort to restore the low spatial frequency components to their original values by energy-filtering and contrast transfer function (CTF) correction (Zhu et al., 1997; Frank, 1997).

Indications of the discrepancy between the volume based on chemical mass and the volume actually occupied come from neutron scattering, which favors a value of 4×10^6 Å^3 (Svergun et al., 1997). The same authors note that the uncorrected density distribution of Stark and coworkers (1995) cannot be reconciled with the shape of the neutron scattering curves, irrespective of the threshold chosen. To explain the wide diversity in volume estimates and measurements, we note that Wittmann (1982) estimated a 10% increase in molecular mass due to associated spermidine and ions. There is uncertainty in the electron microscope

Received for publication 1 May 1997 and in final form 25 August 1997.

Address reprint requests to Dr. Joachim Frank, Wadsworth Center, New York State Department of Health, Empire State Plaza, Box 509, Albany, NY 12201-0509. Tel.: 518-474-7002; Fax: 518-486-2191; E-mail: joachim@wadsworth.org.

0006-3495/98/01/589/06 $2.00

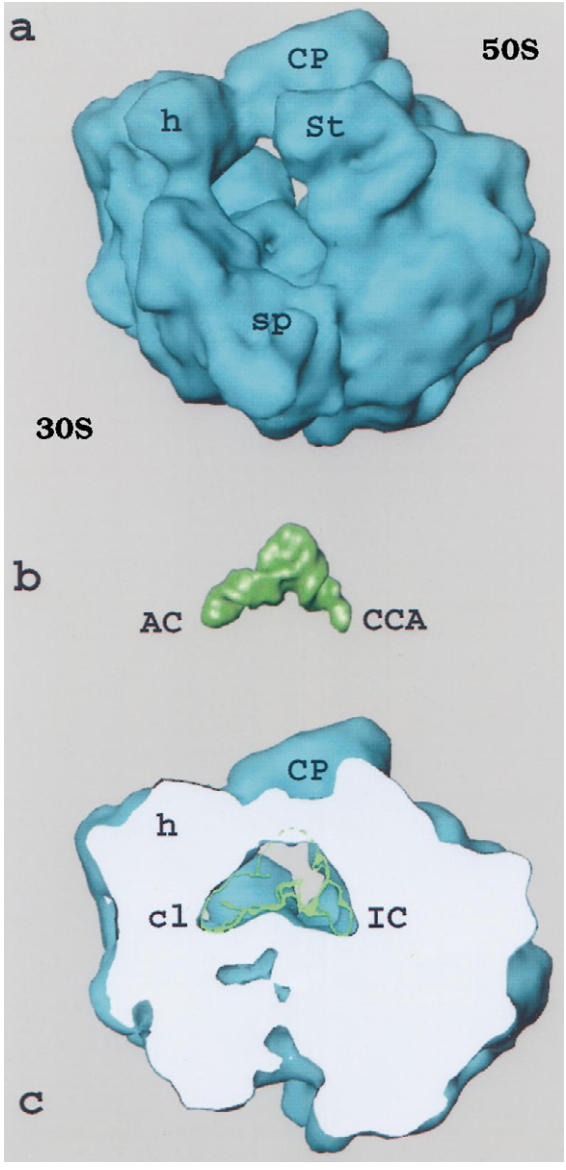

FIGURE 1 Evidence of a close fit between the shapes of the intersubunit space and the tRNA molecule. (*a*) Reconstruction of the ribosome, using a contour that encloses a molecular volume of 4×10^6 Å^3. (*b*) Surface representation of tRNA in an orientation assumed to be likely within the ribosome. AC, anticodon loop; CCA, acceptor end. (*c*) Cross section through the ribosome reconstruction in the same orientation as depicted in the top panel. The outline of tRNA (b) has been superimposed in green. Landmarks: Small subunit: h, head; sp, spur; cl, cleft. Large subunit: CP, central protuberance; St, L7/L12 stalk; IC, interface canyon.

magnification as well, with a 5% variation (a typical value) producing a 15% variation in measured volume. Moreover, the presence of bound water would tend to affect values from neutron scattering and cryo-EM differently. There is, furthermore, a strong dependency of measured volume on the resolution in a cryo-EM reconstruction. All points taken together argue in favor of criteria for the choice of molecular boundary that are independent of volume estimates: continuity of features such as bridges, stalks, etc., and, as the resolution improves, similarity to components known from x-ray crystallography to atomic resolution. In Figs. 2 and 3, a threshold enclosing 3.4×10^6 Å^3 has been used.

SPATIAL ORGANIZATION OF THE INTERSUBUNIT SPACE

Going by the appearance of the intersubunit space (Fig. 1), we are led to view this space as a corridor designed to narrowly constrain the movement of the tRNA molecule along a path that ensures a precisely choreographed sequence of binding events at both ends of the molecule. This succession of binding events is probably assisted by interactions that could actively promote or passively track the movement. Although little is known to date about the precise path followed by the tRNA, the first study describing the direct visualization of tRNA on the ribosome by Agrawal and co-workers (1996) and the one later by Stark and co-workers (1997) have provided evidence of "snug" fitting of the tRNA into its preordained space.

To see the spatial constraints governing the interactions of tRNAs and the ribosome, it is essential to understand the topography of the intersubunit space (ISS). The layout of the ISS can be seen (Fig. 2) by splitting the ribosome into its two subunits along a plane that is roughly perpendicular to the plane of cutting used in Fig. 1. This view shows how the characteristic shape of the ISS is produced by the topographic features of the two subunits in the area where they face each other. We distinguish the ceiling and the floor of the ISS.

The left part (in reference to Fig. 1) of the ceiling is formed by the flat inclined inner wall of the 30S subunit head (Fig. 2, *left*), and the right part is formed by the inclined inner wall of the central protuberance (CP) and, continuous with it, by the wall of the interface canyon (first noted by Radermacher et al., 1987) of the 50S subunit (Fig. 2, *right*). The inclinations of the two walls are such that the angle enclosed is ~90° (Fig. 1 *c*). The 30S subunit head and the 50S subunit central protuberance lean toward each other, forming a narrow contact, so that the precise shape of the ceiling may be maintained.

The floor of the ISS is constituted in large part by the bridge that was first observed by Frank and coworkers (1991), which is formed by the fusion of the platform of the 30S subunit and the lower edge of the interface canyon. It has an elevated ridgelike structure (the "central ridge"), which is mainly contributed by the edge of the 30S platform, situated almost in the middle between the left and right walls, but more toward the L1 end. The floor falls off on either side from the central ridge, toward the 30S subunit on the left and the 50S subunit on the right. The angles of inclination are such that the angle formed between the ramps is close to 270°. The two inclined walls of the floor are roughly parallel to the two walls of the ceiling, with a separation such that the open space accommodates the thickness of the tRNA quite closely. The pockets formed on the two sides of the central ridge are unequal in depth, with

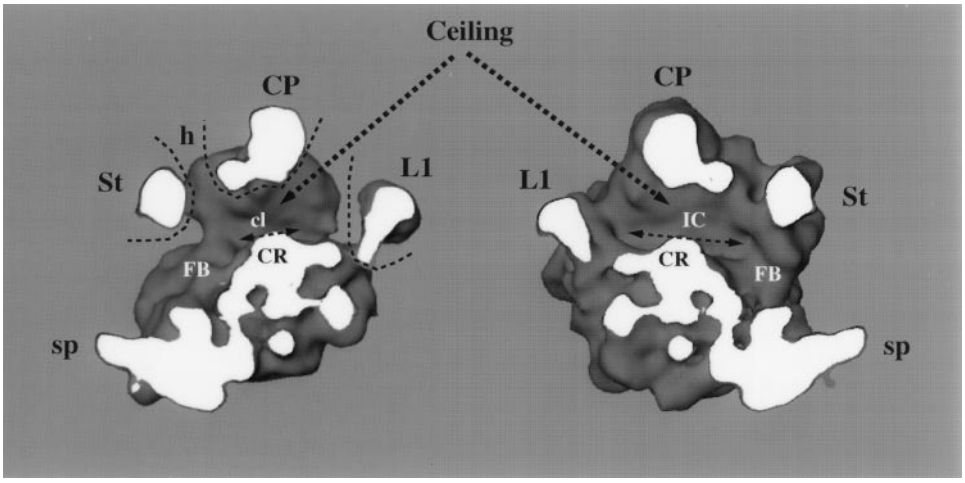

FIGURE 2 Topography of the intersubunit space. The ribosome was separated into its two subunits by a cutting plane that roughly divides the intersubunit space in half. Landmarks: small subunit: h, head; sp, spur; cl, cleft. Large subunit: L1, L1 protein; St, L7/L12 stalk; IC, interface canyon; CP, central protuberance. Joint features: CR, central ridge; FB, factor binding region.

the pocket on the side of the 30S subunit (i.e., the cleft between the platform and the neck) being deeper and more sharply defined than the pocket on the side of the 50S subunit (i.e., the interface canyon), which is rather shallow.

Taken together, the fit between the space formed upon association of the two subunits and the tRNA substrate molecule (as known from x-ray crystallography) is quite remarkable: they agree in linear dimensions (width and depth of the pockets) as well as in angle. Because of the difference in the depth of the two pockets, there is only one general way to fit the L-shaped tRNA structure into this intersubunit space: by placing its long arm that carries the anticodon loop on the side of the small subunit, which in fact is essential for the interaction with the mRNA codons that binds the 30S subunit. However, because the space provided is a corridor that is open on both ends, there is actually an entire continuous range of positions that the tRNA molecule can assume. To make an inventory of possible movements, we bear in mind that the general movement of tRNA is thought to progress from the L7/L12 stalk end of the ribosome toward the L1 protein.

Beginning at the L7/L12 end, the tRNA is able to move toward the L1 end without changing its orientation, except for minor "wiggling" movements that may result from alternating contacts in the two pockets. Another type of movement becomes possible once the elbow of the molecule has passed through the passageway beneath the narrow contact between the subunit heads; it can now pivot around an axis that lies in the plane of the molecule, parallel to its ends. Two pivoting motions are conceivable: one could leave the two ends of the molecule in their place within their respective pockets, so that they serve as pivoting points, and tilt the molecule forward so that the elbow approaches the L1 protein. The other could leave the elbow in contact with the top of the ceiling and let the molecule pivot upward with both ends.

tRNA MOVEMENT IN LIGHT OF EXPERIMENTAL FINDINGS

So far we have gauged the possible movements of the molecule from the existing geometric constraints. The next step would be to introduce well-characterized binding states related to the elongation process. Thus, to characterize the path of the tRNAs, it is necessary to place three known sites within the ribosome, A (aminoacyl), P (peptidyl), and E (exit) sites. Each of these sites (with the possible exception

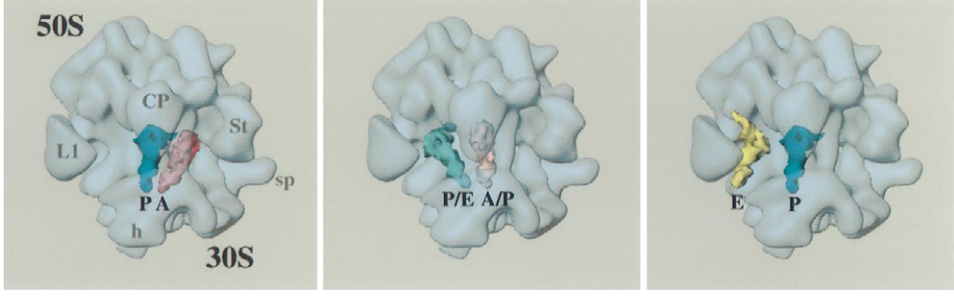

FIGURE 3 Three main stages of the elongation cycle following the hybrid-site model, shown by using a transparent model of the 70S ribosome (*seen from top*). (*Left*) Pretranslocational state, with tRNAs in the A and P sites. (*Middle*) Hybrid or transitional state, with one tRNA in the P/E state, the other in the A/P state. (*Right*) Posttranslocational state in which the ribosome is ready for a new ternary complex, aa-tRNA · EF-Tu · GTP, depicting one tRNA in the P site, the other in the E site. (Positions of A and E sites are adopted from Agrawal et al. (1996).) Landmarks in the left-hand panel are defined as in Fig. 2.

of the E site) involves both the 30S and 50S subunits. Because the mRNA binds to the 30S subunit (Okamoto and Takanami, 1963), the anticodon arm of the tRNAs must always face the 30S subunit. As the peptide bond is formed at the peptidyl transferase center that is located on the 50S subunit (Monro, 1967), the CCA ends carrying the amino acid and the peptidyl chain must face the 50S subunit.

To date, four studies have located the tRNA within the 70S ribosome. Agrawal and co-workers (1996) used the ribosome programmed with poly(U) as mRNA and supplied $tRNA^{Phe}$. Under the buffer conditions used, three tRNAs are known to bind to the ribosome, associated with the A, P, and E sites (Rheinberger et al., 1981). The difference mass observed indeed accounts for most of the volume occupied by three tRNA molecules. In the interpretation of the mass by Agrawal and coworkers, the A- and P-site tRNAs are roughly at expected positions, although the angle between the two tRNAs (in the range of 135°, according to a reevaluation) is in conflict with the florescent resonance energy transfer data (Johnson et al., 1982; Paulsen et al., 1983), which place an upper limit on the distance between the D-loops and would limit the angle to ~60°. The movement from the A- to the P-site position would be along a screw path, involving a rotation of ~135° around the anticodon-CCA axis and a translation along that axis by 10 Å toward the 50S subunit. The E-site tRNA is seen in a peculiar position enclosing the globular L1 protein within the inner bend of its elbow, and its anticodon end still makes contact with the outer edge of the platform of the 30S subunit. The movement from the P-site to the E-site position would again be along a screw, but this time with a nearly 180° rotation and a further translation by ~20 Å toward the 50S subunit.

Experimental evidence from other electron microscopy studies, in which defined mRNAs, acylated tRNAs, and different buffer systems were used (Stark et al., 1997; Agrawal et al., manuscript in preparation), appear to point to a somewhat different position for the P- and E-site tRNAs in pre- and posttranslocational states, with the anticodon of P-site tRNA shifted more toward the L1 end of the ribosome, and in the S-configuration, a constellation postulated by Sundaralingam and co-workers (1975; see model accompanying the presentation of the ribosome reconstruction by Frank et al., 1995b). The main finding, which confirms the placements of the anticodon and amino acid adaptor sites within the intersubunit space on the small and large subunits, respectively, is in basic agreement in all three studies (see also the commentary by Moore, 1997).

Another experimental approach that has been used is proton-spin contrast variation, in which the neutron scattering contrast of a ribosome ligand is varied and the resulting scattering curves are evaluated on the basis of existing models. Using this approach, Wadzack and coworkers (1997) determined the positions of the gravity centers of the complex formed by a small mRNA segment and two tRNAs in the pre- and posttranslocational states. Although not conclusive with regard to the individual tRNA positions, the study shows that the entire complex moves by ~12 Å toward the head of the 30S subunit and toward L1.

EVIDENCE OF MOLECULAR ADAPTATION

Following this first direct evidence of a tight three-dimensional accommodation, it is worth contemplating its evolutionary ramifications. There is little that tRNA alone can accomplish in translating a genetic sequence into a peptide sequence—it is just an oddly shaped molecule that comes in more than 20 essentially different varieties, constituting the elements of an "alphabet soup." Conversely, the ribosome by itself is equally useless for this task, representing a highly complex scaffold ready to accept, when programmed with mRNA, the cognate tRNA molecules through delivery via the EF-Tu · GTP · aa-tRNA ternary complex. Recognizing the complete mutual dependency of the ribosome and tRNA in accomplishing the most elaborate part of protein synthesis, we must assume that these two structures, along with protein factors assisting in initiation, elongation, and termination, have coevolved from simpler ones, following steps of structural evolution that each guaranteed full functionality (see also Dick and Schamel, 1995). It is well known that tRNA genes are located within every ribosomal RNA transcription unit of *E. coli* in the spacer region and/or trailer regions (see review by Gegenheimer and Apirion, 1981). Thus we must see the system formed by tRNA and ribosome as a paradigm of adaptability of living molecules, arguably the oldest in evolutionary terms.

Evidence of adaptability has also been found in two structures closely related to tRNA: EF-G · GDP and the aforementioned ternary complex, EF-Tu · GTP · aa-tRNA appear to be very similar (Nissen et al., 1995; Clark and Nyborg, 1997), a fact that shines light on the close functional relationship between these complexes in the course of the elongation cycle. Mechanistically, elucidation of the elongation cycle poses a fascinating problem: it is by now realized that during this cycle, each end of the tRNA molecule interacts successively with more than one site on both subunits. Only two tRNAs are bound to the ribosome at any given time during the elongation cycle. Because the precise sequence of these interactions and the motor that provides the force of the movements of tRNA and mRNA are as yet poorly understood, we are left with speculation. The group of Knud Nierhaus in Berlin has amassed evidence indicating the presence of allosteric effects that could be instrumental in preventing more than two tRNAs from being present on the ribosome at any time. The observation that the relative protection pattern between these two molecules remains unchanged in the course of translocation led the group to propose the dynamic-domain model (Nierhaus et al., 1995). In that model, the existence of a domain on the large subunit is postulated that binds to both tRNAs and is capable of movement by a substantial distance (in the range of 10 Å), the distance required to advance by one codon to facilitate the transition from the pre- to the posttranslocational state.

Harry Noller's group has proposed the hybrid-site model (Moazed and Noller, 1989), according to which the tRNA moves "one step at a time," always maintaining the binding to one site on one subunit while advancing from one site to the next on the other subunit. In this process, conformational changes of the tRNA may also play an important role (see Yarus and Smith, 1995). A scheme depicting the tRNA ribosome complex in three main stages of the elongation cycle following such a model is shown in Fig. 3.

It is difficult to discuss the pros and cons of these models without reference to the extensive literature on the results of cross-linking and chemical protection studies, which would be beyond the scope of this article. However, a very simple mechanistic argument can be made by considering the geometry of the tRNA interactions with the ribosome. Keeping in mind that the two ends of the molecule are separated by ~75 Å, and that they must make successive binding contacts to sites on both subunits, it is immediately apparent that a mode of transition that allows the molecule to lose contact on both sides would pose a hazard during the transient movement that might lead to complete disruption of the cycle. Given the high reliability of translation (failure rate 1:10,000), it is unlikely that this mode of transition is realized. This plausibility argument supports the general idea of Noller's hybrid-site model, because the characteristic feature of that model is the maintenance of the interaction on one end of the molecule, as the interaction on the other end is severed from one site and established with the next site. However, both higher spatial resolution and time-resolved experiments (see Berriman and Unwin, 1994) may be required to make a conclusive determination.

CONCLUSION

The interaction between tRNA and the ribosome is a prime example of movement and adaptability of biological molecules. We expect that, as strides are being made toward an atomic model of the ribosome, the arguments we have advanced on the basis of a low-resolution morphological description of the ribosome will be increasingly refined by analysis of the time sequence of binding interactions between molecular lock and key.

We thank Yanhong Li and Amy Heagle for assistance with the preparation of the illustrations.

This work was supported, in part, by grants from the National Institutes of Health (1R01 GM29169) and the National Science Foundation (BIR-9219043) (to JF).

REFERENCES

Agrawal, R. K., P. Penczek, R. A. Grassucci, Y. Li, A. Leith, K. H. Nierhaus, and J. Frank. 1996. Direct visualization of A-, P-, and E-site transfer RNAs in the *Escherichia coli* ribosome. *Science.* 271: 1000–1002.

Berriman, J. A., and P. N. T. Unwin, 1994. Analysis of transient structures by cryo-electron microscopy combined with rapid mixing of spray droplets. *Ultramicroscopy.* 56:241–252.

Clark, B. F. C., and J. Nyborg. 1997. The ternary complex of EF-Tu and its role in protein biosynthesis. *Curr. Opin. Struct. Biol.* 7:110–116.

Dick, T. P., and W. A. Schamel. 1995. Molecular evolution of transfer RNA from the precursor hairpins: implications for the origin of protein synthesis. *J. Mol. Evol.* 41:1–9.

Frank, J. 1996. Three-Dimensional Electron Microscopy of Macromolecular Assemblies. Academic Press, San Diego.

Frank, J. 1997. The ribosome at high resolution—the donut takes shape. *Curr. Opin. Struct. Biol.* 7:266–272.

Frank, J., P. Penczek, R. Grassucci, and S. Srivastava. 1991. Three dimensional reconstruction of the 70S *Escherichia coli* ribosome in ice: the distribution of ribosomal RNA. *J. Cell Biol.* 115:597–605.

Frank, J., A. Verschoor, Y. Li, J. Zhu, R. K. Lata, M. Radermacher, P. Penczek, R. Grassucci, R. K. Agrawal, and S. Srivastava. 1995a. A model of the translational apparatus based on a three-dimensional reconstruction of the *Escherichia coli* ribosome. *Biochem. Cell Biol.* 73:757–767.

Frank, J., J. Zhu, P. Penczek, Y. Li, S. Srivastava, A. Verschoor, M. Radermacher, R. Grassucci R. K. Lata, and R. K. Agrawal. 1995b. A model of protein synthesis based on cryo-electron microscopy of the *E. coli* ribosome. *Nature.* 376:441–444.

Gegenheimer, P., and D. Apirion. 1981. Processing of prokaryotic ribonucleic acid. *Microbiol. Rev.* 45:502–541.

Johnson, A. E., H. J. Adkins, E. A. Matthews, and C. R. Cantor. 1982. Distance moved by transfer RNA during translocation from the A site to the P site on the ribosome. *J. Mol. Biol.* 156:113–140.

Moazed, D., and F. Noller. 1989. Intermediate states in the movement of transfer RNA in the ribosome. *Nature.* 342:142–148.

Monro, R. E. 1967. Catalysis of peptide bond formation by 50S ribosomal subunits from *Escherichia coli. J. Mol. Biol.* 26:147–151.

Moore, P. 1995. Ribosomes seen through a glass less darkly. *Structure.* 3:851–852.

Moore, P. 1997. Protein synthesis in slow motion. *Curr. Biol.* 7: R179–R181.

Nierhaus, K. H., D. Beyer, M. Dabrowski, M. A. Schäfer, C. M. T. Spahn, J. Wadzack, J.-U. Bittner, M. Burkhardt, G. Diedrich, R. Jünemann, D. Kamp, H. Voss, and H. B. Stuhrmann. 1995. The elongating ribosome: structural and functional aspects. *J. Biochem. Cell. Biol.* 73:1011–1021.

Nissen, P., M. Kjieldgaard, S. Thirup, G. Polekhina, L. Teshetnikova, B. F. C. Clark, and J. Nyborg. 1995. Crystal structure of the ternary complex of Phe-tRNA(phe), EF-Tu, and a GTP analog. *Science.* 270: 1464–1472.

Okamoto, T., and M. Takanami. 1963. Interaction of ribosomes and natural polyribonucleotides. *Biochim. Biophys. Acta.* 76:266–274.

Paulsen, H., J. M. Robertson, and W. Wintermeyer. 1983. Topological arrangement of two transfer RNAs on the ribosome: fluorescence energy transfer measurements between A and P site-bound $tRNA^{Phe}$. *J. Mol. Biol.* 167:411–426.

Radermacher, M., T. Wagenknecht, A. Verschoor, and J. Frank. 1987. Three-dimensional structure of large ribosomal subunit from *E. coli. EMBO J.* 6:1107–1114.

Rheinberger, H. J., H. Sternbach, and K. H. Nierhaus. 1981. Three tRNA binding sites on *Escherichia coli* ribosomes. *Proc. Natl. Acad. Sci. USA.* 78:5310–5314.

Stark, H., F. Müller, E. V. Orlova, M. Schatz, P. Dube, T. Erdemir, F. Zemlin, R. Brimacombe, and M. Van Heel. 1995. The 70S ribosome at 23 Å resolution: fitting the ribosomal RNA. *Structure.* 3:815–821.

Stark, H., E. V. Orlova, J. Rinke-Appel, N. Jünke, F. Müller, M. Rodnina, W. Wintermeyer, R. Brimacombe, and M. Van Heel. 1997. Arrangement of tRNAs in pre- and posttranslocational ribosomes revealed by electron cryo microscopy. *Cell.* 88:19–28.

Sundaralingam, M., T. Brenman, N. Yathindra, and T. Ichikawa. 1975. Stereochemistry of messenger RNA codon transfer RNA anticodon interaction on the ribosome during peptide bond formation. *In* Structure and Conformation of Nucleic Acids and Protein-Nucleic Acid Interactions. M. Sundaralingam and S. T. Rao, editors. University Park Press, Baltimore. 101–115.

Svergun, D. I., N. Burkhardt, J. S. Pedersen, M. H. J. Koch, V. V. Volkov, M. B. Kazin, W. Meerwinck, H. B. Stuhrmann, G. Diederich, and K. H. Nierhaus. 1997. Solution scattering structural analysis of the 70S *Escherichia coli* ribosome by contrast variation. I. Invariants and validation of electron microscopic models. *J. Mol. Biol.* 271:588–601.

Wadzack, J., N. Burkhardt, R. Jünemann, G. Diedrich, K. H. Nierhaus, J. Frank, P. Penczek, W. Meerwinck, M. Schmitt, R. Willumeit, and H. Stuhrmann. 1997. Direct localization of the tRNAs within the elongating ribosome by means of neutron scattering (proton-spin contrast-variation). *J. Mol. Biol.* 266:343–356.

Wittmann, H. G. 1982. Components of bacterial ribosomes. *Annu. Rev. Biochem. J.* 51:155–183.

Yarus, M., and D. Smith 1995. tRNA on the ribosome: a waggle theory. *In* tRNA: Structure, Biosynthesis and Function. D. Soell and U. Raj Bhandary, editors. ASM Press, Washington, DC. 443–469.

Zhu, J., P. A. Penczek, R. Schröder, and J. Frank. 1997. Three dimensional reconstruction with contrast transfer function correction from energy-filtered cryoelectron micrographs: procedure and application to the 70S *Escherichia coli* ribosome. *J. Struct. Biol.* 118:197–219.